JGR Atmospheres

RESEARCH ARTICLE
10.1029/2023JD038682

Special Section:
Advances in scaling and modeling of land-atmosphere interactions

Validation of Two Newly Developed Albedo Schemes Based on the Observations Over the Region With Evergreen Broadleaved Forest in Southern China

Huan Wang[1,2], Zhigang Wei[1], Anning Huang[2], Xianru Li[1], Li Ma[1], and Shitong Guo[1]

[1]State Key Laboratory of Earth Surface Processes and Resource Ecology, Faculty of Geographical Science, Beijing Normal University, Beijing, China, [2]School of Atmospheric Sciences, Nanjing University, Nanjing, China

Key Points:

- Two new canopy surface albedo schemes considering the influence of solar elevation angle and air relative humidity are proposed
- The new canopy surface albedo schemes can reduce the canopy surface albedo of evergreen broad-leaved forest overestimated by CLM5 model

Correspondence to:
Z. Wei and A. Huang,
wzg@bnu.edu.cn;
anhuang@nju.edu.cn

Citation:
Wang, H., Wei, Z., Huang, A., Li, X., Ma, L., & Guo, S. (2024). Validation of two newly developed albedo schemes based on the observations over the region with evergreen broadleaved forest in Southern China. *Journal of Geophysical Research: Atmospheres*, *129*, e2023JD038682. https://doi.org/10.1029/2023JD038682

Received 9 FEB 2023
Accepted 14 DEC 2023

Abstract Existing land surface models still have large error in the simulation of surface albedo. At present, introducing the influence of meteorological factors into the albedo parameterization scheme is an effective way to improve the albedo simulation. However, the improvement of the vegetation canopy surface albedo parameterization scheme is still insufficient. Therefore, based on the radiation and meteorological observation data during 1 November 2015–30 April 2018 from a land-atmosphere interaction observation tower in a typical secondary evergreen broadleaved forest in Southern China, this study firstly analyzed the influencing factors of canopy surface albedo. It was found that the solar elevation angle and air relative humidity are two key factors influencing the canopy surface albedo, and the impact of the solar elevation angle on canopy surface albedo is not exactly the same on diurnal and seasonal scales. Then, two new canopy surface albedo parameterization schemes of additive form and multiplicative form were proposed and introduced into CLM5 model for single point simulation. Results show that the adoption of newly developed canopy surface albedo parameterization schemes can improve the simulation of diurnal and seasonal variations of albedo and reduce the overestimation of the simulation of near-infrared radiation albedo and visible radiation albedo in the CLM5 model, then significantly reduce the root mean square errors of reflected solar radiation and net radiation simulation.

Plain Language Summary Surface albedo is an important factor affecting the heat exchange between land and atmosphere, and is critical for weather forecasting and regional climate modeling. At present, even in some complex land surface models, the canopy surface albedo parameterization scheme only considers the variation of leaf and stem index and the cosine of the solar zenith angle over time but does not take into account the effect of meteorological factors. In this study, two newly developed canopy albedo schemes that take into account the effects of solar elevation angle and air relative humidity were developed, and then introduced into the CLM5 model for single point simulation. The results show that the new canopy albedo scheme can indeed improve the simulation skills of the reflected solar radiation. The results emphasize the important influence of meteorological factors on the surface albedo, and the findings may provide a base to further develop and improve the CLM5 model.

1. Introduction

Since the 1980s, people have realized that climate is not only formed by the thermal and dynamic processes of the atmosphere, but is also the result of interactions with the biosphere, hydrosphere and lithosphere (Huang et al., 2013; Liu et al., 2021; Pielke, 2001). Land-atmosphere interactions are an important part of these processes, and surface albedo is an important factor affecting the heat exchange between land and atmosphere, which represents the reflection ability of the land surface to the solar radiation. Any slight change in the underlying surface will cause a change in its albedo, which affects the surface's absorption of solar radiation and the surface's transport of longwave radiation to the atmosphere, thus affecting the dynamic and thermal conditions near the surface, and finally lead to a change in the local weather and climate (Dirmeyer et al., 2006; Gash & Shuttleworth, 1991; Irvine et al., 2011; Lee et al., 2011; Li et al., 2018; Liang et al., 2010; Sedlar et al., 2011). It has been shown that a 0.01 shift in surface albedo will result in an energy change of 3.4 $W \cdot m^{-2}$, which is about 1.5∼5 times more powerful than carbon dioxide in changing global surface temperature (Jorgensen et al., 2014; Wielicki et al., 2005). Therefore, surface albedo has become a parameter of great interest in numerical models, whether in land surface models, weather forecast models, or regional climate models.

In current land surface models, the surface albedo is obtained by weighted summation based on different types of land cover, such as bare soil, snow surface and vegetation. However, since the calculation process includes many empirical parameters and approximate processing, the albedo simulation still has a large deviation, leading to the estimation of surface radiation balance and heat balance is not ideal, which is one of the reasons for the poor accuracy of climate simulation (Baldocchi et al., 2000; Xiao et al., 2011). At present, the simulation surface albedo relative error of most global circulation models is generally between 5% and 15% (Ding & Sun, 2006). Consequently, it is critical to improve the surface albedo simulation skill in land surface models, and hence to improve the simulation performance of weather forecast models and regional climate models (Betts & Ball, 1997; Dickinson, 1995; Dai et al., 2003; Liang et al., 2005; Rotenberg & Yakir, 2010; Wei et al., 2016).

Through conducting near-surface observation experiments, obtaining the radiation and albedo information under different underlying surface conditions in different regions is an important means to optimize the albedo parameterization scheme in land surface models. Many studies have shown that the surface albedo is affected by various factors, such as the solar elevation angle, soil water content, soil color, vegetation coverage, surface roughness, and so on, and has obvious characteristic differences in different areas with different underlying surface conditions at different times (Guan et al., 2009; Liu et al., 2008; Roxy et al., 2010; Sugathan et al., 2014; Zheng et al., 2015). Based on the previous field observation experiments, it is generally believed that the bare surface albedo is exponentially (linearly) with the solar elevation angle (soil moisture content) decreases. For the underlying surface with vegetation coverage (such as farmland, shrubs and grassland), the higher vegetation coverage corresponds to the lower surface albedo (Bao et al., 2008; Cai et al., 2012; Tian et al., 2018; Zhang & Huang, 2004; Zheng et al., 2014). Introducing these factors into the albedo scheme in land surface models can obviously improve the accuracy of albedo calculation (Kala et al., 2014; Liang et al., 2005; Loarie et al., 2011; Wang et al., 2007; Yang et al., 2008; Zheng et al., 2017). However, previous studies on the improvement of albedo parameterization schemes are mostly focused on bare soil and vegetation coverage great changed areas, few researches have paid attention to evergreen broad-leaved forests.

Southern China has a wide distribution of subtropical evergreen broadleaf forests. The accuracy of canopy surface albedo simulation of evergreen broad-leaved forest in land surface models will further affect the simulation accuracy of regional climate model for monsoon intensity, spatial distribution of precipitation and relevant continent-scale circulation (Xue et al., 2004). However, even in some complex land surface models, the canopy surface albedo parameterization scheme only considers the changes of leaf and stem index and the cosine of solar zenith angle over time but does not consider the influence of other meteorological factors, nor can it well simulate the canopy surface albedo of evergreen broad-leaved forest, especially on hourly and monthly scales (Barlage et al., 2015; Berbet & Costa, 2003; Dickinson, 1983; Oleson et al., 2008, 2010; Yanagi & Costa, 2011; Zhu et al., 2019). In warm and humid subtropical evergreen broad-leaved forests, vegetation coverage is high and changes little throughout the year, so soil exposure is low. The most current surface albedo parameterization schemes, which considered the influence of vegetation coverage change and soil moisture, are not applicable over these areas. Therefore, observations and further research should be intensified in subtropical evergreen broadleaf forest areas.

We established a land-atmosphere interaction observation tower in the Phoenix Mountain forest of Zhuhai, Guangdong Province, where the underlying surface type is the evergreen broad-leaved forest (Wei et al., 2016). The canopy surface albedo and its influencing factors have been systematically studied, and two new albedo parameterization schemes were proposed based on field observations and introduced into Community Land Model Version 5 (CLM5). To what extent the newly developed albedo parameterization schemes affect the performance of the CLM5 model in simulating the canopy surface albedo and surface radiation balance and related possible causes have been systematically explored in this study. Findings may provide a base to further develop and improve the CLM5 model over the regions with evergreen broad-leaved forest in Southern China.

2. Data, Model and Experimental Design, Method

2.1. Field Observation Data

The field observations used in this study are derived from the land-atmosphere interaction observation tower station in Phoenix Mountain, Zhuhai City, Guangdong Province, China. Figure 1 shows the geographical location of the observation station. It is located at 22°21 '15.5 "N, 113°31' 34.2" E, and 38.5 m above sea level, belonging

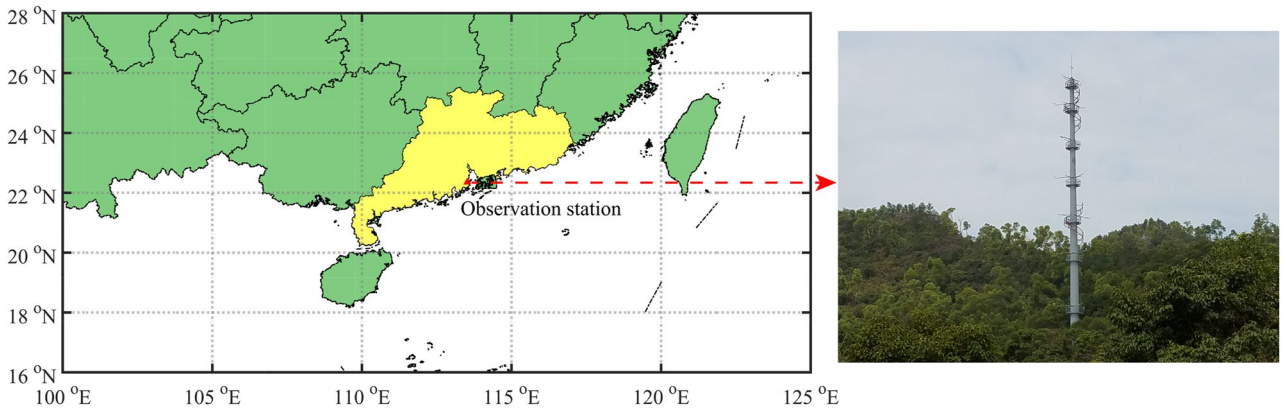

Figure 1. Location of the land-atmosphere interaction observation station in Phoenix Mountain, Zhuhai City, Guangdong Province, China.

to the subtropical monsoon climate zone, so the climate is warm and humid. The underlying surface type is evergreen broad-leaved forest with an average canopy height of 18 m and a forest canopy slope of approximately 5°. In August 2014, the land-atmosphere interaction observation tower station was completely built, and after a two-month trial operation and commissioning, official observations began in November of the same year, and then stopped in May 2018. It has three sets of observation systems: meteorological, radiation and flux. All observation instruments were calibrated by the manufacturer before observation, and the relevant technical parameters are shown in Table 1 (Wang et al., 2021; Wei et al., 2016).

The radiation observation system is set up at 47.5 m, which mainly observes upward and downward solar shortwave radiation (SR), visible radiation (VIS) and ultraviolet radiation (UVR). Meteorological observation instruments are installed on several tower platforms at different heights above and below the forest canopy. All data is recorded every half-hour using local time. Due to the inevitable damage to the surrounding forest during the construction of the observation tower, the observation data used in this study include radiation observation data at 47.5 m and air temperature, air relative humidity, wind speed, pressure, precipitation observation data at 25 m near the canopy height from 1 November 2015 to 30 April 2018 after a one-year recovery period of the forest. Before the study, all observation data have been checked for spatiotemporal consistency, logical extremum and rigid values, and the data that failed to pass the check were corrected or eliminated (Wang et al., 2008, 2021). Due to the thunderstorm and gale weather in summer, the instrument failed, therefore, the observation data from July to August in 2016 and 2017 were missing. The missing data were filled by interpolating the data at the adjacent time. In addition, since there is no radiometer that can directly observe the upward and downward near-infrared radiation (NIR, 0.7~2.8 μm) in the radiation observation system, the near-infrared radiation was obtained by subtracting the visible radiation with the waveband of 0.4~0.7 μm and ultraviolet radiation with the waveband of 0.28~0.4 μm from the solar shortwave radiation with the waveband of 0.285~2.800 μm (Zheng et al., 2012).

Table 1
Observation Instruments for the Solar Radiation Experiment and Their Technical Parameters

Parameter	Instrument name	Instrument model	Measuring range	Observation accuracy
Short wave radiation	Short Wave Radiation Sensor	CMP21	285~2,800 nm	±1.4%
Visible radiation	Optical Quantum Radiation Sensor	SQ-130-L-10	400~700 nm	±5%
Near-infrared radiation	Ultraviolet Radiometer	CUV5	280~400 nm	±5%
Longwave radiation	Long Wave Radiation Sensor	CGR 4	4,500~42,000 nm	±3%
Rainfall	Rain Gauge	TB4MM	0~700 mm/hr	< 250 mm/hr: ±2%
				250~300 mm/hr: ±3%
Relative humidity	Relative Humidity Sensor	HMP155A	0.8~100%	±1.0%
Temperature	Temperature Sensor	HMP155A	−80°C~60°C	±1.0°C

2.2. Model

Community Land Model (CLM) is the land portion for the Community Earth System Model (CESM), and the CLM5 we used in this study is the latest version (https://www.cesm.ucar.edu/models/cesm2/land). CLM5 is one of the most advanced land surface models in the world (Lawrence et al., 2019). It comprehensively considers the physical, hydrological, biochemical and material cycle processes of the land surface and adds many new sub-models to make the land surface process more complete. In the CLM5 model, the two-steam approximation method for calculating atmospheric radiation transmission is introduced into the calculation of vegetation canopy radiation transmission (Dickinson, 1983; Oleson et al., 2008, 2010). As shown in the following basic equations of radiation transfer (Equations 1 and 2), the model divides the transmission process into three parts: extinction, primary scattering and multiple scattering. By assuming the upward and downward diffusion fluxes are completely isotropic, the canopy radiative transfer equations are solved by parametrizing the individual single scattering rate of leaves at the upper and lower boundary conditions of the vegetation canopy. Through complex derivation, the upward and downward radiation fluxes of vegetation with only scattered radiation and only direct radiation can be obtained. Thus, the overall canopy surface albedo, transmittance and absorption rate can be calculated (Zhou et al., 2008).

$$-\overline{\mu}\frac{dI\uparrow}{d(L+S)} + [1-(1-\beta)\omega]I\uparrow - \omega\beta I\downarrow = \omega\overline{\mu}K\beta_0 e^{-K(L+S)} \tag{1}$$

$$\overline{\mu}\frac{dI\downarrow}{d(L+S)} + [1-(1-\beta)\omega]I\downarrow - \omega\beta I\downarrow = \omega\overline{\mu}K(1-\beta_0)e^{-K(L+S)} \tag{2}$$

where $I\uparrow$ and $I\downarrow$ refer to the upward and downward diffuse radiative flux per unit incident radiant flux, respectively. $\overline{\mu}$, ω, β, β_0, and K are vegetation optical parameters, L and S indicate leaf and stem area index, respectively.

2.3. Experimental Design

In this study, three single point simulation experiments with the CLM5 model adopting different canopy surface albedo parameterization schemes were designed and carried out. The CLM5 model is driven by the field meteorological observation data during 1 January 2016 to 31 December 2017, and a $0.1^\circ \times 0.1^\circ$ grid at a center point of 22.35°N, 113.53°E with an underlying surface type of evergreen broadleaved forest is set as the simulation area. The simulations in 2016 are regarded as the adjustment model operation, and the simulations in 2017 are used as the main analysis data to evaluate the ability of the CLM5 model with different canopy surface albedo schemes in simulating the albedo and the reflected solar radiation. The parameterization schemes of canopy surface albedo adopted in the three simulation experiments are: the original albedo scheme (CLMO), the newly proposed albedo scheme in the form of addition (CLMA), and the newly developed albedo scheme in the form of multiplication (CLMM). The details of two newly developed canopy surface albedo parameterization schemes are given in Section 3.2.

2.4. Method

The root mean square error (RMSE) between the simulated value and the observed data is used to evaluate the model simulation ability. The specific formula is as follows:

$$\mathrm{RMSE} = \left[\frac{1}{N}\sum_{i=1}^{N}(S_i - O_i)^2\right]^{1/2} \tag{3}$$

where S_i and O_i are the simulated and observed values, respectively, and N is sample of the time series.

Besides, the Taylor score (TS) is also used in this paper to evaluate the simulation of canopy surface albedo variation trend and amplitude. The calculation formula is as follows (Taylor, 2001):

$$\mathrm{TS} = \frac{4*(1+r)}{\left(SDR + \frac{1}{SDR}\right)^2(1+r_0)} \tag{4}$$

$$r = \frac{\frac{1}{N}\sum_{i=1}^{N}\left(S_i - \overline{S}\right)*\left(O_i - \overline{O}\right)}{\sigma_s\sigma_o} \tag{5}$$

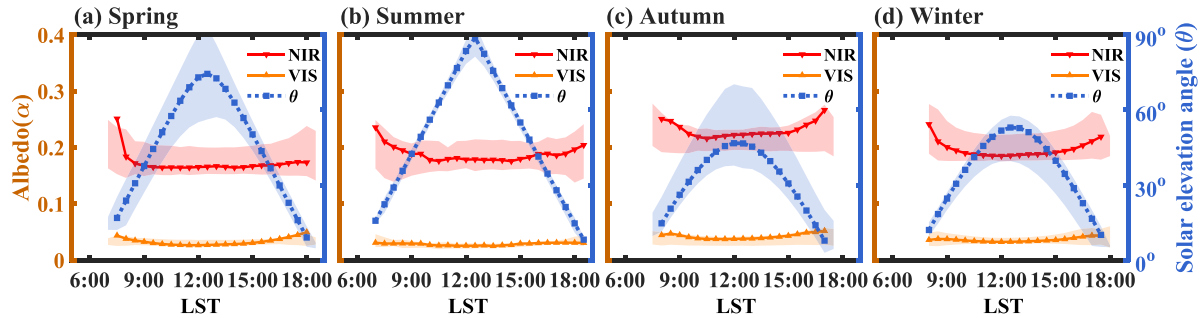

Figure 2. Diurnal variation of canopy surface albedo for near infrared and visible radiation and solar elevation angle in different seasons (The shaded areas represent the 95% confidence intervals).

$$SDR = \frac{\sigma_s}{\sigma_o} \tag{6}$$

$$\sigma_s = \left[\frac{1}{N}\sum_{i=1}^{N}\left(S_i - \overline{S}\right)^2\right]^{1/2} \tag{7}$$

$$\sigma_o = \left[\frac{1}{N}\sum_{i=1}^{N}\left(O_i - \overline{O}\right)^2\right]^{1/2} \tag{8}$$

The r represents the correlation between simulated values and observed values, and r_0 is the theoretical maximum correlation coefficient between the two, which is set as 1 here. And SDR represents the ratio of standard deviation of simulated values (σ_s) to standard deviation of observed values (σ_o). Finally, the $\overline{S}$ and $\overline{O}$ represent the average of simulated and observed values.

3. Results

3.1. Relationship Between the Canopy Surface Albedo and Influencing Factors

In the CLM5 model, the solar shortwave radiation is only divided into near-infrared radiation (wavelength > 0.7 μm) and visible radiation (wavelength < 0.7 μm) with equal proportions, and calculate the albedos of near-infrared radiation and visible radiation are respectively. Therefore, the observed ultraviolet radiation is included into the visible radiation for the subsequent study of albedo parameterization scheme.

In the forested areas, where the relationship between the soil water content and the canopy surface albedo is not obvious, other meteorological factors such as near canopy surface air relative humidity, air temperature, and wind speed may affect the canopy surface albedo (Zhang, 2012; Zhao et al., 2014). Correlation analysis between the canopy surface albedo and meteorological factors showed that the canopy surface albedo is well correlated with the solar elevation angle, air relative humidity and temperature. Through further partial correlation analysis by control variables, it was found that the correlation coefficient between the canopy surface albedo and the solar elevation angle can reach approximately −0.5. While the air relative humidity is still correlated well with the canopy surface albedo, but the correlation coefficient between air temperature and canopy surface albedo becomes very small, which may be caused by the high correlation between air temperature and solar elevation angle. Therefore, the solar elevation angle and air relative humidity are two key factors that have relatively greater impact on the canopy surface albedo.

In previous research, we found that albedo showed obvious diurnal and seasonal variations (Wang et al., 2021). Are the effects of solar elevation angle and air relative humidity on albedo consistent at the diurnal and seasonal scales? To answer this question, this study first randomly selected a day from spring, summer, autumn and winter and revealed the influence of the solar elevation angle on albedo by comparing their diurnal variation relationship (Figure 2). It was found that the albedo presents a "U"-shaped variation with large values in the morning and evening and small values at noon. However, the diurnal variation of the solar elevation angle is exactly opposite

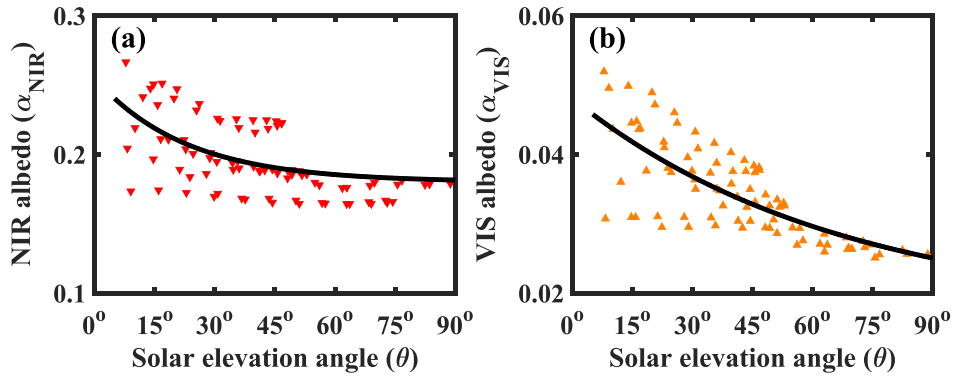

Figure 3. The relationship between the solar elevation angle and canopy surface albedo of near infrared and visible radiation at sub-daily scale.

to the canopy surface albedo. Figure 3 shows the relationship between canopy surface albedo and the solar elevation angle at the sub-daily scale. It can be seen that the canopy surface albedo gradually decreases with the increase of the solar elevation angle, and the decreasing amplitude also gradually decreases with the increase of the solar elevation angle. When the solar elevation angle is greater than 60°, the albedo of the canopy surface to near-infrared radiation does not change with the solar elevation angle, and when the solar elevation angle is greater than 75°, the albedo of the canopy surface to visible radiation does not change with the solar elevation angle. This is in accordance with the diurnal variation of albedo and the solar elevation angle. When the solar elevation angle is small (large), the diurnal variation of albedo is obvious (unobvious).

Similarly, the relationship between canopy surface albedo and solar elevation angle at the seasonal scale can also be indicated by comparing the relationship between them. To exclude the influence of diurnal variation, we calculated the radiation albedo and the corresponding maximum midday solar elevation angle every day during the observation period. As shown in Figure 4, there is also an opposite seasonal variation between the albedo and the maximum midday solar elevation angle. Figure 5 further shows the relationship between the albedo and the maximum midday solar elevation angle. The elevation angle at noon in the evergreen broad-leaved forest area ranges from 45° to 90° in a year. When the solar elevation angle is approximately 45°, it corresponds to winter, at this time, with the increase of the solar elevation angle, the albedo does not change significantly. When the solar elevation angle is greater than 60°, it corresponds to autumn, spring and summer, and the albedo decreases gradually with the increasing of solar elevation.

As mentioned above, although the canopy surface albedo is affected by the solar elevation angle on both diurnal and seasonal scales, it is not completely identical. The canopy surface albedo decreases exponentially with the increase of the solar elevation angle on the diurnal scale, and decreases in a quadratic power form with the increase of the maximum midday solar elevation angle on the seasonal scale. In addition, the same comparative experiment also took place on the relationship between air relative humidity and albedo, and it was found that the diurnal variation of the above variables was sometimes the same and sometimes the opposite, without obvious correlation, while the seasonal variation showed an obvious opposite relationship, the canopy surface albedo

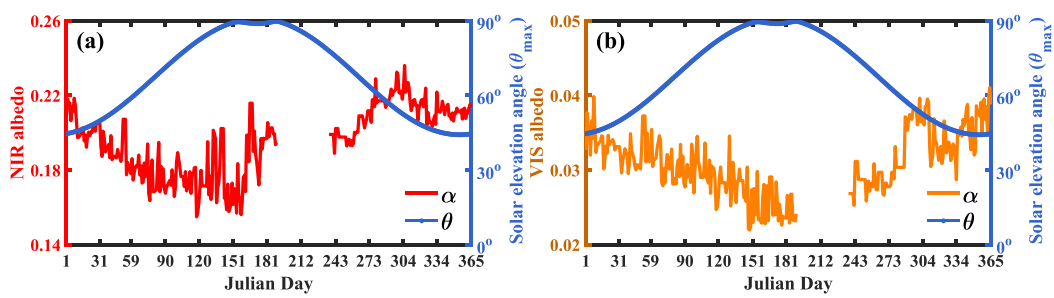

Figure 4. Seasonal variation of canopy surface albedo for the near infrared and visible radiation and solar elevation angle at noon.

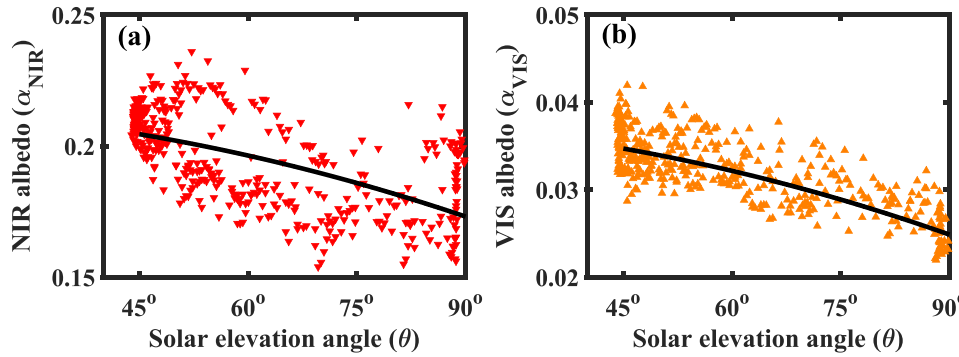

Figure 5. The relationship of the solar elevation angle with the canopy surface albedo of near infrared and visible radiation at noon during the whole observation period with available observations.

decreases linearly with the increase of the air relative humidity (not shown). In summary, the solar elevation angle and air relative humidity are two variables dominating the albedo, and the influence of the solar elevation angle on canopy surface albedo is not completely the same on diurnal and seasonal scales.

3.2. New Albedo Parameterization Schemes

Based on the above relationship between the canopy surface albedo and the influencing factors, we have proposed two new albedo parameterization schemes in the form of addition and multiplication, respectively. For the additive albedo parameterization scheme, it based on the observed annual mean albedo, then superimposed the effects of diurnal and seasonal variations of the solar elevation angle and air relative humidity in the form of addition. The following empirical relationship equations were obtained by fitting:

$$\alpha_{VIS} = 0.0164 * \exp(-0.0178 * \theta) - 1.0906 * 10^{-6} * \theta_m^2 - 0.00005 * rh + 0.034 \quad (9)$$

$$\alpha_{NIR} = 0.0496 * \exp(-0.0179 * \theta) - 4.6075 * 10^{-6} * \theta_m^2 - 0.0001 * rh + 0.199 \quad (10)$$

where α_{VIS} and α_{NIR} represent the albedo of visible radiation and near-infrared radiation on the canopy surface, respectively. θ(degree) is the solar elevation angle, θ_m(degree) is the maximum midday solar elevation angle, and rh (%) is the air relative humidity near the canopy surface, 0.034 and 0.199 are the observed average albedo of visible radiation and near-infrared radiation, respectively. The correlation coefficients of the albedos calculated by Equations 9 (10) with the observations is 0.73 (0.65), and the confidence intervals are both above 90%.

Different from the additive albedo parameterization scheme, which is completely depends on the observed data, the multiplicative albedo parameterization scheme is based on the simulated albedo of CLM5 and approximates the real albedo by multiplying the correction factor. In the original albedo parameterization scheme of CLM5, the influence of the solar elevation angle on the albedo is considered by introducing the cosine of the solar zenith angle, but it is not comprehensive. Replace the cosine of the solar zenith angle in the original scheme by the sine of the maximum midday solar elevation angle. At this time, the simulated albedo only includes the influence of the seasonal variation of the solar elevation angle. Based on the simulated albedo, the influence of the diurnal variation of solar elevation angle and seasonal variation of air relative humidity on the albedo were introduced by multiplying the correction coefficients. The empirical formulas of the multiplication form were obtained as follows:

$$\alpha_{VIS} = \alpha_{VIS}^1 * \exp\left(-0.2073 * \sin\left(\theta * \frac{\pi}{180}\right)\right) * \left(1 - 0.2359 * \left(\frac{rh}{100}\right)\right) * 0.8560 \quad (11)$$

$$\alpha_{NIR} = \alpha_{NIR}^1 * \exp\left(-0.0459 * \sin\left(\theta * \frac{\pi}{180}\right)\right) * \left(1 - 0.1278 * \left(\frac{rh}{100}\right)\right) * 1.0675 \quad (12)$$

where α_{VIS} and α_{NIR} represent the albedo of visible radiation and near-infrared radiation on the canopy surface. α_{VIS}^1 *and* α_{NIR}^1 are the albedo of visible radiation and near-infrared radiation at noon simulated by the original albedo scheme in the CLM5 model with the daily maximal solar elevation angle. θ(degree) is the solar elevation

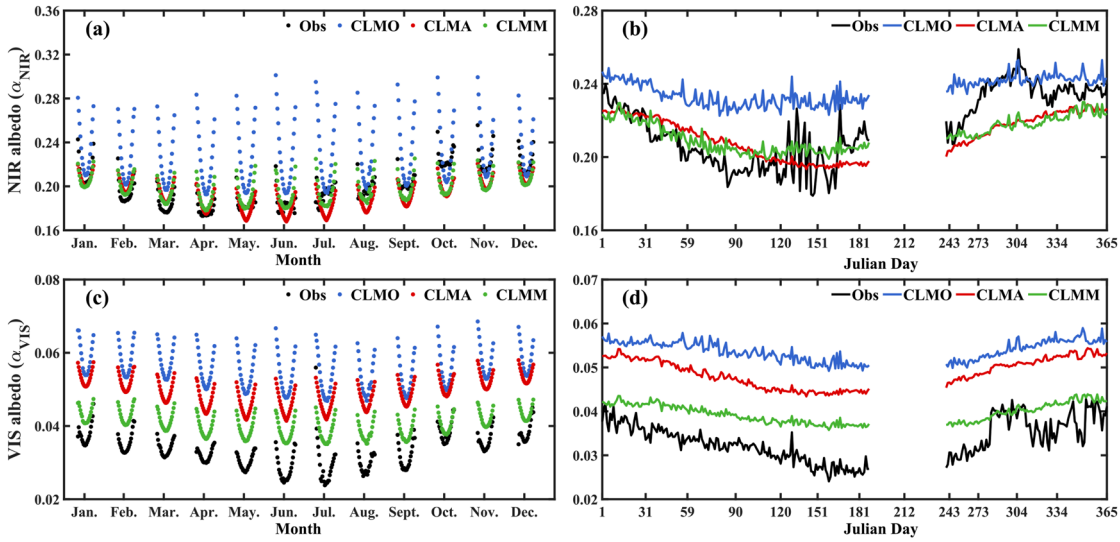

Figure 6. The diurnal variation of canopy surface albedo for the near-infrared and visible radiation from the simulations (obtained from CLMO, CLMA, and CLMM) and observations in each month (a and c) and the seasonal variation of the daily mean canopy surface albedo for the near-infrared and visible radiation from the simulations and observations (b and d).

angle, and *rh* (%) is the air relative humidity near the canopy surface. The correlation coefficient of the albedos calculated by Equation 11 (12) with the observations is 0.63 (0.66), and the confidence intervals are both above 90%.

3.3. Evaluation of Simulations

We introduced the two newly developed albedo parameterization schemes into the CLM5 model to evaluate their performance on the canopy surface radiation energy balance simulation. See Section 2.3 for specific model Settings.

Figure 6 shows the diurnal and seasonal variation of the observed and simulated canopy surface albedo. From Figures 6a and 6c, all three experiments can reproduce the observed diurnal variations of near-infrared and visible radiation albedos that decrease from morning to noon and then increase from noon to evening. However, compared with the observed values, the daily range of canopy surface albedo simulated by the CLMO experiment is too large, especially for the near-infrared radiation albedo. The simulated canopy surface albedos produced by the CLMA and CLMM experiments are much closer to observation compared to the CLMO experiment. As shown in Figures 6b and 6d, the observed canopy surface albedo also shows an obvious seasonal variation: decreasing gradually from winter to spring and increasing gradually from summer to autumn. The seasonal variation of albedo simulated by the CLMO experiment, is much smaller than the observation (Figures 6b and 6d). Compared to the CLMO experiment, the CLMA and CLMM experiments can better simulate the seasonal variation daily-averaged albedo.

As shown in Figures 6a and 6b, the canopy surface albedo of near-infrared radiation simulated by the CLMO experiment is significantly higher than the observation, but in winter the simulated albedo is closer to the observed albedo than at other seasons. However, the albedo simulated by CLMA and CLMM experiments is lower (higher) than observed albedo in autumn and winter (spring and summer), and the simulated albedo is closer to the observed albedo in spring and summer than in the autumn and winter. From the RMSE and TS values (Figures 7a–7c), the RMSE of CLMA and CLMM experimental simulated canopy surface albedos and observed albedo is significantly reduced compared with CLMO experiment, with a reduction of more than 50% (except in October), and the TS is also significantly increased (except in winter). According to the statistics of the whole year's data, it was found that the CLMA and CLMM experiments with the adoption of newly developed albedo schemes can reduce the RMSE from 0.038 to 0.017 and 0.018, respectively.

From Figures 6c and 6d, the canopy surface albedo of visible radiation simulated by the three experiments are significantly larger than the observation. Similarly, using the new canopy surface albedo schemes in the additive form (CLMA) and multiplicative form (CLMM) can significantly reduce the RMSE between the simulated and

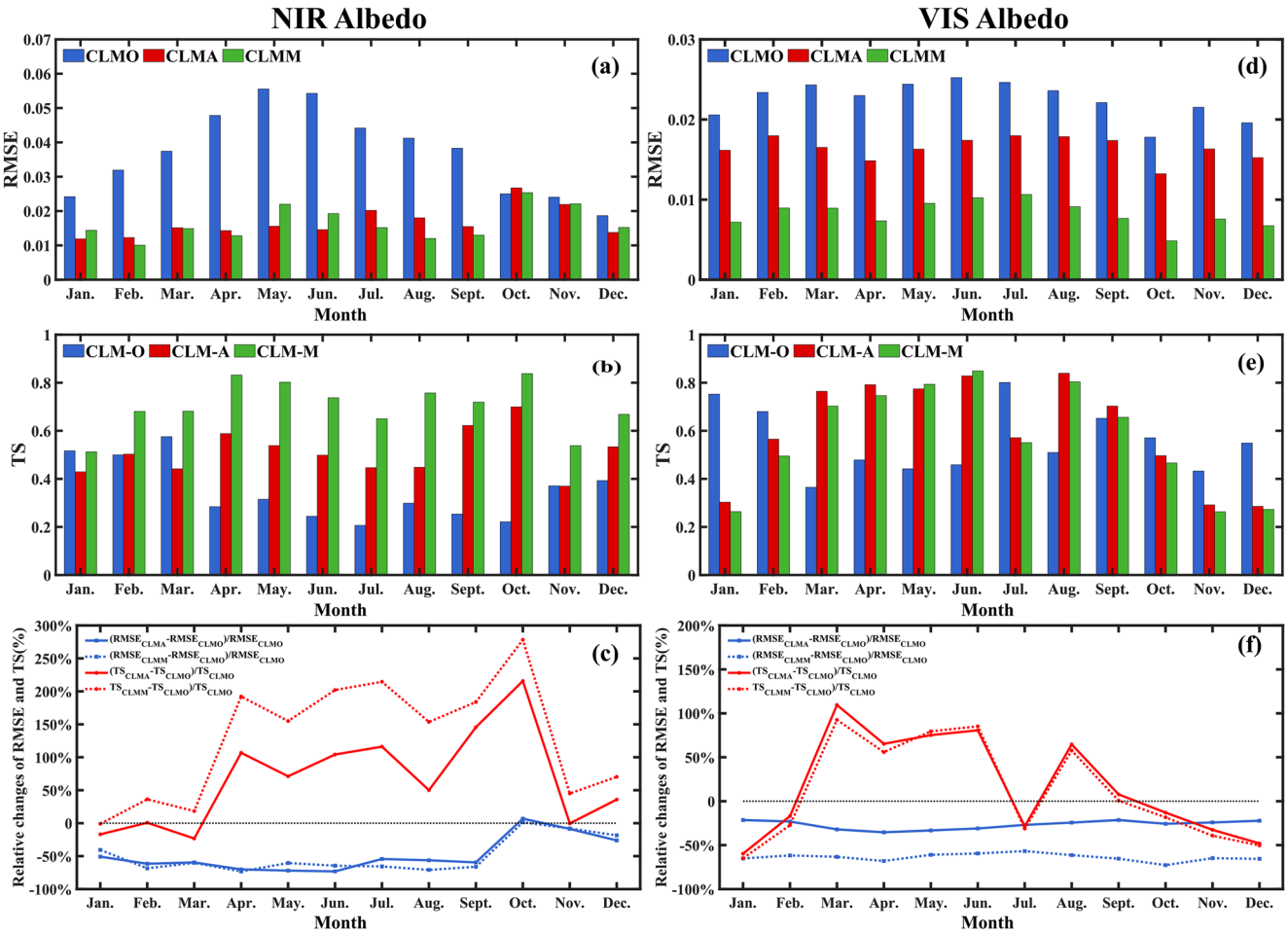

Figure 7. The RMSE and TS of the modeled canopy surface albedo for the near-infrared radiation (a and b) and visible radiation (d and e) in each month. And the relative variation of RMSE and TS of the modeled canopy surface albedo obtained from the CLMA and CLMM compared with the CLMO (c and f).

observed albedos by more than 25% and 50%, respectively (Figures 7d–7f). And the TS value also increased significantly (except in winter). According to the statistics of the whole year's data, it was found that the CLMA and CLMM experiments with the adoption of newly developed albedo schemes can reduce the RMSE from 0.022 to 0.016 and 0.008, respectively.

The new canopy surface albedo schemes in additive and multiplicative form can significantly improve the simulation of the near-infrared radiation albedo and visible radiation albedo in CLM5. Furthermore, they can also significantly improve the simulation of reflected solar radiation and net radiation. According to the diurnal variation and seasonal variation of the difference between simulated reflected solar radiation and observation (Figures 8a and 8b), CLMA and CLMM can reduce the overestimation of reflected solar radiation by CLMO (except in winter). From Figures 9a and 9c, the RMSE of CLMA and CLMM experimental simulated reflected solar radiation and observation also significantly reduced more than 50% compared with CLMO experiment (except in Winter). It is worth noting that the reflected solar radiation simulated by the CLMO experiment is the closest to the observation in winter, which is related to the actual proportion of near-infrared radiation in solar shortwave radiation in winter is more than 50% (Wang et al., 2021). Statistics show that the RMSE of reflected solar radiation simulated by CLMO can be reduced from 6.89 $W \cdot m^{-2}$ to 4.34 $W \cdot m^{-2}$ and 5.60 $W \cdot m^{-2}$ by CLMA and CLMM.

From Figures 8c and 8d, by the diurnal variation trend of the difference between simulated and observed net radiation, we found that the simulated net radiation of the three experimental schemes is often larger than the observed value at night, smaller than the observed value in the day, and the deviation between simulated and observed net radiation at noon is large. The net radiation simulated by CLMA and CLMM can significantly

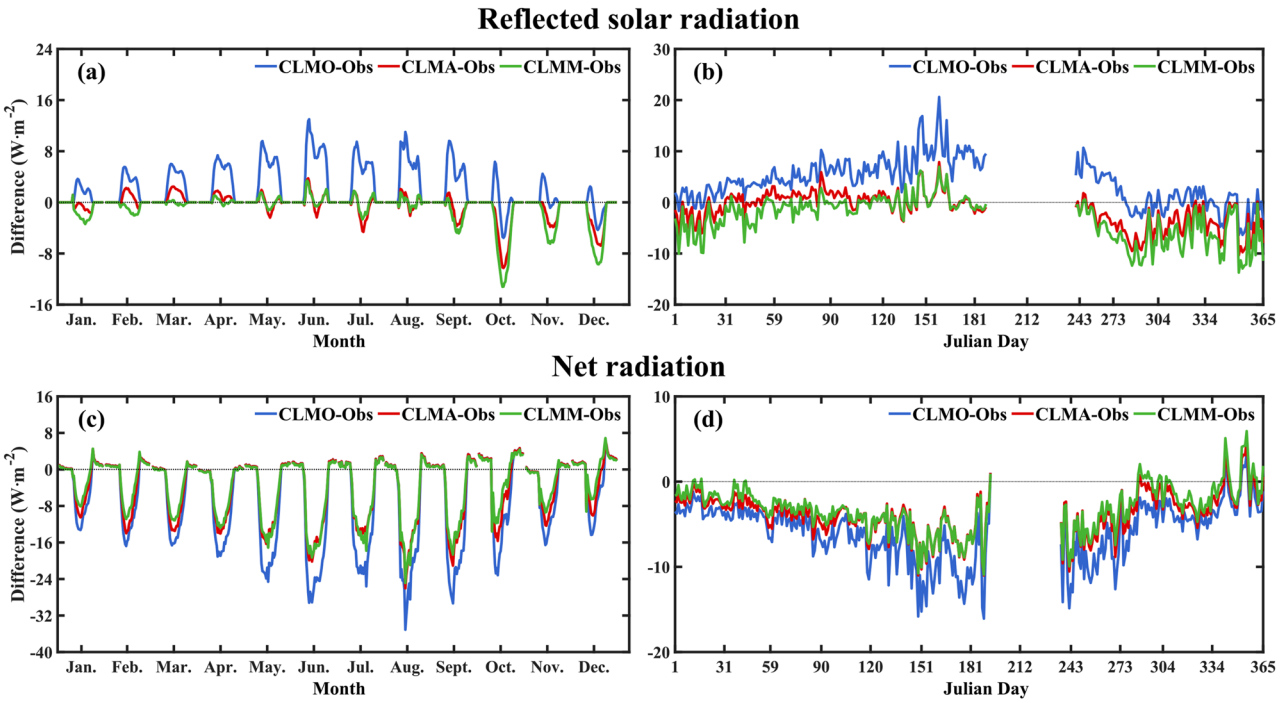

Figure 8. The diurnal variation of the difference between reflected solar radiation and net radiation simulations (obtained from CLMO, CLMA, and CLMM) and observations in each month (a and c). And the seasonal variation of the difference between the daily mean reflected solar radiation and net radiation simulations and observations (b and d).

reduce the underestimate of daytime net radiation simulated by CLMO experiments. The increase in the accuracy of daytime net radiation simulation will also have an impact on nighttime net radiation. The net radiation simulated by CLMA and CLMM can also slightly reduce the overestimation of nighttime net radiation by CLMO experiments. From the perspective of seasonal variation of daily-averaged net radiation, the simulated net radiation is smaller than the observation, and the deviation is larger in summer and autumn, but smaller in winter and spring. From Figures 9b and 9d, the RMSE of CLMA and CLMM experimental simulated net radiation and

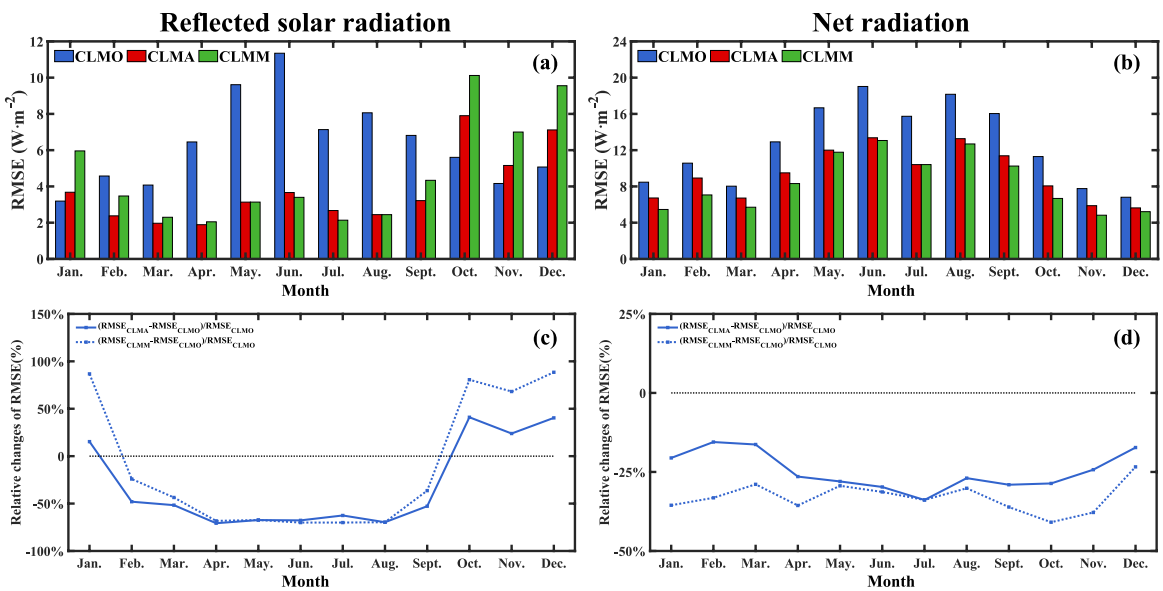

Figure 9. The RMSE of the modeled reflected solar radiation and net radiation simulations in each month (a and b). And the relative variation of the RMSE of the modeled reflected solar radiation and net radiation simulations obtained from the CLMA and CLMM compared with the CLMO (c and d).

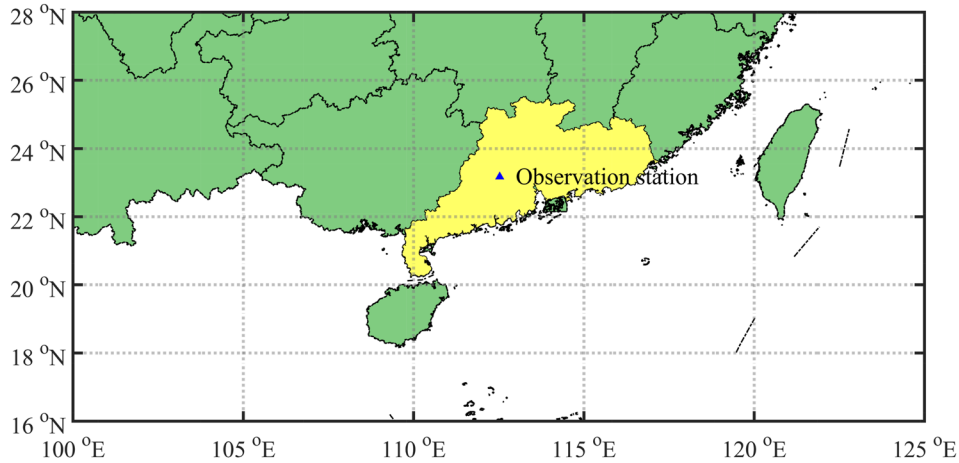

Figure 10. Location of the Dinghushan forest ecosystem research station in Guangdong Province, China.

observation also significantly reduced more than 20% compared with the CLMO experiment. Statistics show that the RMSE of net simulated by CLMO can be reduced from 12.85 W·m^{-2} to 9.41 W·m^{-2} and 8.60 W·m^{-2} by CLMA and CLMM.

3.4. Validation of the Newly Developed Albedo Schemes at Another Site

The observation data for the validation of the newly developed albedo schemes is from the Dinghushan forest ecosystem research station in Guangdong Province, China (Figure 10). It is located at 23°10'25.4" N, 112°32'3.7"E, and the underlying surface is also a subtropical evergreen broad-leaved forest (Liu et al., 2020). We select the solar shortwave radiation and reflected radiation data in 2010 as the analysis data. Similarly, we used CLM5 model with different albedo schemes to conduct simulation experiments from 2009 to 2010 (CLMO, CLMA, CLMM), and the simulations in 2010 are used as the main analysis data for comparative analysis. The driving data used for the simulation is from the China Meteorological Forcing Dataset, with a spatial resolution of 0.1 and a temporal resolution of 3 hr (Yang et al., 2019).

Figure 11 shows the seasonal variation of the observed and simulated canopy surface albedo. It can be seen that, similar to Zhuhai station, the albedo of solar radiation simulated by the CLMO experiment is significantly greater than the observed albedo, while the simulations of CLMA and CLMM experiments are closer to the observation, and the seasonal variation of the albedo simulated by the CLMM experiment is closer to the observation. From

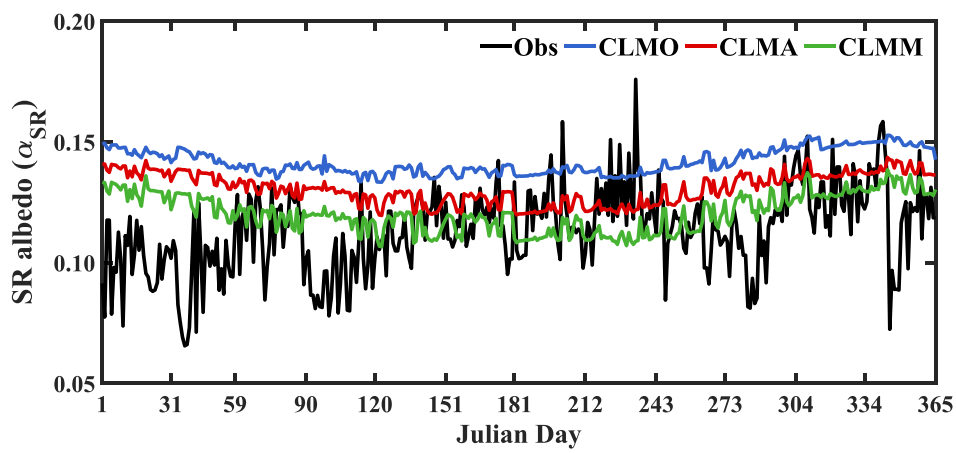

Figure 11. The seasonal variation of the daily mean canopy surface albedo for the solar shortwave radiation from the simulations (obtained from CLMO, CLMA, and CLMM) and observations in Dinghushan Station.

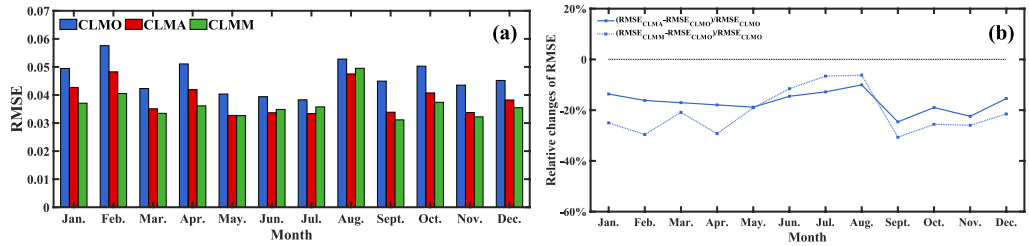

Figure 12. The RMSE of the modeled albedo of solar radiation obtained from the CLMA, CLMM and CLMO in each month (a), and the relative variation of the RMSE of the modeled albedo of solar radiation obtained from the CLMA and CLMM compared with the CLMO (b).

Figures 12a and 12b, the RMSE of CLMA and CLMM experimental simulated canopy surface albedos and observed albedo are significantly reduced compared with CLMO experiment, with a reduction similar to 30% (except in summer). According to the statistics of the whole year's data, it was found that the CLMA and CLMM experiments with the adoption of newly developed albedo schemes can reduce the RMSE from 0.033 to 0.027 and 0.026, respectively.

4. Conclusions

Through conducting near-surface observation experiments, obtaining land surface information under different underlying surface conditions in different regions and exploring land surface process mechanisms are important means for optimizing the parameterization scheme in land surface models. The Southern China is widely distributed with evergreen broad-leaved forest. Based on the radiation and meteorological observation data from the observation tower, this study analyzed the relationships between canopy surface albedo and potential influencing factors, and then proposed two new albedo parameterization schemes, which were introduced into the land surface model CLM5 to improve the model performance, main findings are listed as follows.

1. The solar elevation angle and air relative humidity are the two variables dominating the canopy surface albedo, and the impact of solar elevation angle on albedo is not exactly the same on the diurnal and seasonal scales.
2. Two new canopy surface albedo parameterization schemes in the additive and multiplicative forms were further established. The additive albedo parameterization scheme is superimposed the effects of diurnal and seasonal variations of the solar elevation angle and air relative humidity on the observed annual mean albedo. The multiplicative albedo parameterization scheme is based on the simulated albedo of CLM5 and approximates the real albedo by multiplying the correction factor.
3. The new canopy albedo parameterization schemes can not only improve the simulation of diurnal and seasonal variations of albedo, but also significantly reduce the overestimation of visible radiation albedo and near-infrared radiation albedo in the CLM5 model with the original albedo scheme, and thereafter lead to obvious improvements in the simulation of reflected solar radiation and net radiation.

Although the albedo parameterization schemes proposed in current study obviously improved the canopy surface albedo and reflected solar radiation simulation in the evergreen broadleaved forest, it still has their shortcomings and limitations, and needs to be further improved. Firstly, the newly developed albedo schemes are obtained by fitting the observation data over the evergreen broadleaved forest area and has not been verified on other forest areas. The additive albedo parameterization scheme is based on the observed annual mean albedo, so it can be extended to other forest underlying surfaces by establishing the relationship between NDVI and the mean vegetation albedo. The multiplicative albedo parameterization scheme is to multiply the original simulated value by correction factors to obtain the albedo value, so the different correction factors can be given for different vegetation types. Secondly, the albedo parameterization schemes developed in this study was only introduced into the CLM5 model for single-point simulation and was not introduced into the regional climate model to study its effect on regional climate simulation. Finally, the proposed albedo parameterization schemes only considered the effects of solar elevation angle and air relative humidity on albedo, while the effects of clouds and precipitation on the radiation reaching the surface were not considered. Clouds and aerosols can affect the proportion of scattered and direct, near-infrared and visible radiation in the short wave radiation reaching the canopy surface through absorption and scattering of solar radiation, and this effect needs to be described more accurately in the

model. Therefore, the current albedo parameterization scheme needs further verification and promotion, and the addition of more influencing factors, to consider more weather conditions in order to further improve its simulation ability.

Data Availability Statement

The observation data from the land-atmosphere interaction observation tower station in Zhuhai Phoenix Mountain (Wei, 2023) and Dinghushan forest ecosystem research station in Guangdong Province (Liu et al., 2020) were used in this study. The driving data used in the model simulations is China Meteorological Forcing Dataset (Yang et al., 2019). Software—The source codes of Community Earth System Model Version 2.1.3 used in this study are freely available online (Danabasoglu et al., 2020).

Acknowledgments
This study is supported by State Key Laboratory of Earth Surface Processes and Resource Ecology (2022-GS-01) and National Natural Science Foundation of China (41875089). The work was carried out at National Supercomputer Center in Tianjin, and the calculations were performed on TianHe-1(A).

References

Baldocchi, D., Kelliher, F. M., Black, T. A., & Jarvis, P. (2000). Climate and vegetation controls on boreal zone energy exchange. *Global Change Biology*, *6*(S1), 69–83. https://doi.org/10.1046/j.1365-2486.2000.06014.x

Bao, Y., Lü, S., Zhang, Y., Meng, X., & Yang, S. (2008). Improvement of surface albedo simulations over arid regions. *Advances in Atmospheric Sciences*, *25*(3), 481–488. https://doi.org/10.1007/s00376-008-0481-y

Barlage, M., Tewari, M., Chen, F., Miguez-Macho, G., Yang, Z.-L., & Niu, G.-Y. (2015). The effect of groundwater interaction in North American regional climate simulations with WRF/Noah-MP. *Climatic Change*, *129*(3–4), 485–498. https://doi.org/10.1007/s10584-014-1308-8

Berbet, M. L. C., & Costa, M. H. (2003). Climate change after tropical deforestation: Seasonal variability of surface albedo and its effects on precipitation change. *Journal of Climate*, *16*(12), 2099–2104. https://doi.org/10.1175/1520-0442(2003)016<2099:ccatds>2.0.co;2;2

Betts, A. K., & Ball, J. H. (1997). Albedo over the boreal forest. *Journal of Geophysical Research*, *102*(D24), 28901–28909. https://doi.org/10.1029/96jd03876

Cai, F., Zhou, G. S., Ming, H. Q., & Ming, H. Q. (2012). A simulative study of effects of dynamic parameterization of surface albedo on land-atmosphere flux exchanges: A case study of rainfed maize field in northeast China. *Acta Meteorologica Sinica*, *70*(5), 1149–1164. https://doi.org/10.1007/s11783-011-0280-z

Dai, Y., Zeng, X., Dickinson, R. E., Oleson, K. W., Bonan, G. B., Bosilovich, M. G., et al. (2003). The common land model. *Bulletin of the American Meteorological Society*, *84*(8), 1013–1024. https://doi.org/10.1175/BAMS-84-8-1013

Danabasoglu, G., Lamarque, J.-F., Bacmeister, J., Bailey, D. A., DuVivier, A. K., Edwards, J., et al. (2020). The community earth system model version 2 (CESM2). *Journal of Advances in Modeling Earth Systems*, *12*, e2019MS001916. https://doi.org/10.1029/2019MS001916

Dickinson, R. E. (1983). Land surface processes and climate-surface albedos and energy balance. *Advances in Geophysics*, *25*, 305–353. https://doi.org/10.1016/S0065-2687(08)60176-4

Dickinson, R. E. (1995). Land-atmosphere interaction. *Reviews of Geophysics*, *33*(S2), 917–922. https://doi.org/10.1029/95RG00284

Ding, Y. H., & Sun, Y. (2006). Recent advances in climate change science. *Advances in Climate Change Research*, *2*(4), 161–167. https://doi.org/10.3969/j.issn.1673-1719.2006.04.003

Dirmeyer, P. A., Gao, X., Zhao, M., Guo, Z., Oki, T., & Hanasaki, N. (2006). Gswp-2: Multimodel analysis and implications for our perception of the land surface. *Bulletin of the American Meteorological Society*, *87*(10), 1381–1398. https://doi.org/10.1175/BAMS-87-10-1381

Gash, J. H., & Shuttleworth, W. J. (1991). Tropical deforestation: Albedo and the surface-energy balance. *Climatic Change*, *19*(1), 123–133. https://doi.org/10.1007/BF00142219

Guan, X., Huang, J., Guo, N., Bi, J., & Wang, G. (2009). Variability of soil moisture and its relationship with surface albedo and soil thermal parameters over the Loess Plateau. *Advances in Atmospheric Sciences*, *26*(4), 692–700. https://doi.org/10.1007/s00376-009-8198-0

Huang, R., Zhou, D., & Chen, W. (2013). Recent progress in studies of air–land interaction over the arid area of Northwest China and its impact on climate. *Chinese Journal of Atmospheric Sciences*, *37*(2), 189–210. https://doi.org/10.1016/j.scienta.2012.12.020

Irvine, P. J., Ridgwell, A., & Lunt, D. J. (2011). Climatic effects of surface albedo geoengineering. *Journal of Geophysical Research*, *116*(D24), a–n. https://doi.org/10.1029/2011JD016281

Jorgensen, S. V., Cherubini, F., & Michelsen, O. (2014). Biogenic CO_2 fluxes, changes in surface albedo and biodiversity impacts from establishment of a miscanthus plantation. *Journal of Environmental Management*, *146*(dec.15), 346–354. https://doi.org/10.1016/j.jenvman.2014.06.033

Kala, J., Evans, J. P., Pitman, A. J., Schaaf, C. B., Decker, M., Carouge, C., et al. (2014). Implementation of a soil albedo scheme in the cablev1.4b land surface model and evaluation against modis estimates over Australia. *Geoscientific Model Development*, *7*(5), 1671–2140. https://doi.org/10.5194/gmd-7-2121-2014

Lawrence, D. M., Fisher, R. A., Koven, C. D., Oleson, K. W., Swenson, S. C., Bonan, G., et al. (2019). The community land model version 5: Description of new features, benchmarking, and impact of forcing uncertainty. *Journal of Advances in Modeling Earth Systems*, *11*(12), 4245–4287. https://doi.org/10.1029/2018MS001583

Lee, X. H., Michael, L., Goulden, D. Y., Barr, A., Black, T. A., Bohrer, G., et al. (2011). Observed increase in local cooling effect of deforestation at higher latitudes. *Nature*, *479*(7373), 384–387. https://doi.org/10.1038/NATURE10588

Li, Q. P., Ma, M. G., Wu, X. D., & Yang, H. (2018). Snow cover and vegetation-induced decrease in global albedo from 2002 to 2016. *Journal of Geophysical Research: Atmospheres*, *123*(1), 124–138. https://doi.org/10.1002/2017jd027010

Liang, S., Wang, K., Zhang, X., & Wild, M. (2010). Review on estimation of land surface radiation and energy budgets from ground measurement, remote sensing and model simulations. *IEEE Journal of Selected Topics in Applied Earth Observations and Remote Sensing*, *3*(3), 225–240. https://doi.org/10.1109/JSTARS.2010.2048556

Liang, X. Z., Xu, M., Gao, W., Kunkel, K., Slusser, J., Dai, Y., et al. (2005). Development of land surface albedo parameterization based on Moderate Resolution Imaging Spectroradiometer (MODIS) data. *Journal of Geophysical Research*, *110*(D11). https://doi.org/10.1029/2004JD005579

Liu, H., Wang, B., & Fu, C. (2008). Relationships between surface albedo, soil thermal parameters and soil moisture in the semi-arid area of Tongyu, northeastern China. *Advances in Atmospheric Sciences*, *25*(5), 757–764. https://doi.org/10.1007/s00376-008-0757-2

Liu, P., Zhang, Q., & Liu, X. D. (2020). A meteorological dataset observed by Dinghushan forest ecosystem research station (2005–2018) [dataset]. Chinese Scientific Data, *5*(4). https://doi.org/10.11922/csdata.2020.0016.zh

Liu, W. C., Zhang, Q., & Liu, X. W. (2021). The impact of land-atmosphere interaction on the initiation and development of convective activities: A review. *Plateau Meteorology*, *40*(6), 1278–1293. https://doi.org/10.7522/j.issn.1000-0534.2021.zk0019

Loarie, S. R., Lobell, D. B., Asner, G. P., Mu, Q., & Field, C. B. (2011). Direct impacts on local climate of sugar-cane expansion in Brazil. *Nature Climate Change*, *1*(2), 105–109. https://doi.org/10.1038/nclimate1067

Oleson, K. W., Lawrence, D. M., & Bonan, G. B. (2010). *Technical description of version 4.0 of the community land model(CLM)*. National Center for Atmospheric Research.

Oleson, K. W., Niu, G. Y., Yang, Z. L., Lawrence, D. M., Thornton, P. E., Lawrence, P. J., et al. (2008). Improvements to the Community Land Model and their impact on the hydrological cycle. *Journal of Geophysical Research*, *113*(G1). https://doi.org/10.1029/2007jg000563

Pielke, R. A. (2001). Influence of the spatial distribution of vegetation and soils on the prediction of cumulus Convective rainfall. *Reviews of Geophysics*, *39*(2), 151–177. https://doi.org/10.1029/1999RG000072

Rotenberg, E., & Yakir, D. (2010). Contribution of semi-arid forests to the climate system. *Science*, *327*(5964), 451–454. https://doi.org/10.1126/science.1179998

Roxy, M. S., Sumithranand, V. B., & Renuka, G. (2010). Variability of soil moisture and its relationship with surface albedo and soil thermal diffusivity at astronomical observatory, Thiruvananthapuram, south Kerala. *Journal of Earth System Science*, *119*(4), 507–517. https://doi.org/10.1007/s12040-010-0038-1

Sedlar, J., Tjernström, M., Mauritsen, T., Shupe, M. D., Brooks, I. M., Persson, P. O. G., et al. (2011). A transitioning Arctic surface energy budget: The impacts of solar zenith angle, surface albedo and cloud radiative forcing. *Climate Dynamics*, *37*(7–8), 1643–1660. https://doi.org/10.1007/s00382-010-0937-5

Sugathan, N., Biju, V., & Renuka, G. (2014). Influence of soil moisture content on surface albedo and soil thermal parameters at a tropical station. *Journal of Earth System Science*, *123*(5), 1115–1128. https://doi.org/10.1007/s12040-014-0452-x

Taylor, K. E. (2001). Summarizing multiple aspects of model performance in a single diagram. *Journal of Geophysical Research*, *106*(D7), 7183–7192. https://doi.org/10.1029/2000JD900719

Tian, L., Chen, J. Q., & Shao, C. L. (2018). Interdependent dynamics of LAI-albedo across the roofing landscapes: Mongolian and Tibetan plateaus. *Remote Sensing*, *10*(7), 1159. https://doi.org/10.3390/rs10071159

Wang, H., Wei, Z., Liu, Y., Liu, Y., & Li, X. (2021). Solar spectral albedo characteristics over a typical secondary evergreen broadleaf forest in the Lingnan area in China. *Theoretical and Applied Climatology*, *145*(3–4), 1075–1087. https://doi.org/10.1007/s00704-021-03688-9

Wang, S., Trishchenko, A. P., & Sun, X. (2007). Simulation of canopy radiation transfer and surface albedo in the ealco model. *Climate Dynamics*, *29*(6), 615–632. https://doi.org/10.1007/s00382-007-0252-y

Wang, S., Zhang, Q., & Zhang, H. (2008). Characteristics of surface albedo and soil heat conductivity in sparse vegetation site (in Chinese). *Journal of Desert Research*, *28*(1), 119–124. https://doi.org/10.3724/SP.J.1011.2008.00323

Wei, Z., Hu, J., & Dong, W. (2016). Basic observations and diurnal variation of key meteorological variables on clear days in the Phoenix Mountain area of Zhuhai. *Chinese Journal of Atmospheric Sciences*, *40*(2), 423–436. https://doi.org/10.3878/j.issn.1006-9895.1503.15111

Wei, Z. G. (2023). Observation data from the Phoenix mountain in Zhuhai [dataset]. Zenodo. https://doi.org/10.5281/zenodo.8053826

Wielicki, B. A., Bruce, A., Wong, T., Priestley, K. P., Priestley, K., & Kandel, R. (2005). Changes in earth's albedo measured by satellite. *Science*, *308*(5723), 825. https://doi.org/10.1126/science.1106484

Xiao, D., Tao, F., & Moiwo Juana, P. (2011). Research progress on surface albedo under global change. *Advances in Earth Science*, *26*(11), 1217–1224. https://doi.org/10.1007/s00376-010-1000-5

Xue, Y., Juang, H.-M. H., Li, W.-P., Prince, S., DeFries, R., Jiao, Y., & Vasic, R. (2004). Role of land surface processes in monsoon development: East Asia and West Africa. *Journal of Geophysical Research*, *109*(D3), D03105. https://doi.org/10.1029/2003JD003556

Yanagi, S. N., & Costa, M. H. (2011). Simulations of tropical rainforest albedo: Is canopy wetness important? *Anais da Academia Brasileira de Ciências*, *83*(4), 1171–1180. https://doi.org/10.1590/s0001-37652011005000047

Yang, F., Mitchell, K., Hou, Y. T., Dai, Y., Zeng, X., Wang, Z., & Liang, X.-Z. (2008). Dependence of land surface albedo on solar zenith angle: Observations and model parameterization. *Journal of Applied Meteorology and Climatology*, *47*(11), 2963–2982. https://doi.org/10.1175/2008JAMC1843.1

Yang, K., He, J., Tang, W., Lu, H., Qin, J., Chen, Y., & Li, X. (2019). China meteorological forcing dataset (1979-2018) [Dataset]. A Big Earth Data Platform for Three Poles. https://doi.org/10.11888/AtmosphericPhysics.tpe.249369.file

Zhang, Q., & Huang, R. H. (2004). Parameters of land-surface processes for Gobi in north-west China. *Boundary-Layer Meteorology*, *110*(3), 471–478. https://doi.org/10.1023/B:BOUN.0000007224.08804.b8

Zhang, X. Z. (2012). The responses of surface albedo to climatic changes in xilin gol grassland. *Geographical Research*, *13*(3), 374–382. https://doi.org/10.3724/SP.J.1047.2011.00374

Zhao, Z. Z., Zhao, K., Xu, J. B., Xiao, Z.-F., Cui, J.-F., Hong, Z., et al. (2014). Spatial-temporal changes of surface albedo and its relationship with climate factors in the source of three rivers region. *Arid Zone Research*, *31*(06), 1031–1038. https://doi.org/10.13866/j.azr.2014.06.08

Zheng, Z., Dong, W., Li, Z., Zhao, W., Hu, S., Yan, X., et al. (2015). Observational study of surface spectral radiation and corresponding albedo over Gobi, desert, and bare loess surfaces in northwestern China. *Journal of Geophysical Research: Atmospheres*, *120*(3), 883–896. https://doi.org/10.1002/2014JD022516

Zheng, Z., Wei, Z., & Li, Z. (2014). Study of parameterization of surface albedo of bare soil over the gobi desert in the Dunhuang region. *Chinese Journal of Atmospheric Sciences*, *38*(2), 297–308. https://doi.org/10.3878/j.issn.1006-9895.2013.13147

Zheng, Z., Wei, Z., Li, Z., & Wang, C. (2012). Characteristics of solar spectral radiation and albedo during early autumn in Dunhuang Gobi (in Chinese). *Acta Energiae Solaris Sinica*, *33*(11), 1937–1943. https://doi.org/10.1038/aps.2012.149

Zheng, Z., Wei, Z., Wen, Z., Dong, W., Li, Z., Wen, X., et al. (2017). Inclusion of solar elevation angle in land surface albedo parameterization over bare soil surface. *Journal of Advances in Modeling Earth Systems*, *9*(8), 3069–3081. https://doi.org/10.1002/2017MS001109

Zhou, W. Y., Guo, P. W., & Luo, Y. (2008). A study on the radiative transfer parameterization scheme within canopy in land surface process model. *Acta Meteorologica Sinica*, *66*(3), 359–370. https://doi.org/10.3724/SP.J.1047.2008.00014

Zhu, Y. Z., Zhang, L. H., Tan, X. Y., Zhu, Y., Han, Z., & He, C. (2019). Evaluation of simulation performance of CLM4. 5 at the Yanchi Station in the agricultural-pastoral ecotone of Northwest China. *Journal of Arid Meteorology*, *37*(3), 430–438.